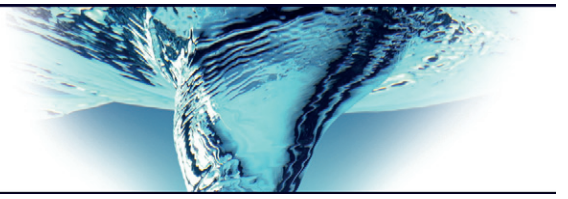
J. Fluid Mech. (2014), *vol.* 752, R1, doi:10.1017/jfm.2014.354



JFM RAPIDS
journals.cambridge.org/rapids

A continuum approach to predicting electrophoretic mobility reversals

Robert F. Stout and Aditya S. Khair†

Department of Chemical Engineering, Carnegie Mellon University, Pittsburgh, PA 15213, USA

(Received 7 May 2014; revised 12 June 2014; accepted 18 June 2014;
first published online 4 July 2014)

We present a continuum approach to predicting the electrophoretic mobility of a charged dielectric colloidal particle in a concentrated multivalent electrolyte. Our model takes into account steric (excluded volume) hindrance between ions via Bikerman's approach (*Philos. Mag.*, vol. 33, 1942, p. 384) and ion–ion electrostatic (Coulombic) correlations via the work of Bazant *et al.* (*Phys. Rev. Lett.*, vol. 106, 2011, 046102). The latter can result in the prediction of an electrophoretic mobility reversal, that is, the migration velocity of a particle switches direction with increasing ion concentration. Our model predictions compare favourably with experiments that observe mobility reversals in multivalent electrolytes.

Key words: colloids, low-Reynolds-number flows, micro-/nano-fluid dynamics

1. Introduction

Electrophoresis refers to the motion of a charged colloidal-scale particle in an electrolytic solution under an applied electric field. Electrophoretic transport is used extensively in analytical chemistry (Elbashir & Aboul-Enein 2013), microfluidics (Squires & Quake 2005) and DNA sequencing (Dorfman 2010). A central quantity of interest is the electrophoretic mobility, which relates the migrative velocity of a charged particle, $\boldsymbol{U}$, to the uniform applied field, $\boldsymbol{E}_\infty$. The electrophoretic mobility for a uniformly charged spherical colloid is a scalar quantity (M_e), such that $\boldsymbol{U} = M_e\boldsymbol{E}_\infty$ (Russel, Saville & Schowalter 1989).

Charged surfaces and particles in electrolytic solutions attract a diffuse region of net charge around them – a 'Debye layer'. In dilute solutions, the thickness of this layer is characterized by the Debye length, κ^{-1}: for a binary electrolyte $\kappa^{-1} = \sqrt{\varepsilon k_B T/e^2 n_+^\infty z_+(z_+ - z_-)}$, where ε is the dielectric permittivity, k_B is the Boltzmann constant, T is temperature, e is the fundamental charge, n_+^∞ is the bulk number density of counterions, and z_+ and z_- are the charge numbers of the counter and coions, respectively, assuming a negatively charged surface. For a

† Email address for correspondence: akhair@andrew.cmu.edu

© Cambridge University Press 2014

https://doi.org/10.1017/jfm.2014.354 Published online by Cambridge University Press

1 mM monovalent salt at $T = 298$ K, $\kappa^{-1} \approx 10$ nm. Thus, for a colloidal particle of radius $R \sim O$ (μm), $\kappa R \gg 1$ and the Debye layer is said to be 'thin'.

In this thin-Debye-layer limit, $M_e = \varepsilon\zeta/\eta$ (where η is solution viscosity), as shown by Smoluchowski (1903) for a uniformly charged dielectric spherical particle with a surface 'zeta' potential (ζ) that is small compared with the thermal voltage, $k_BT/e \simeq 25$ mV. Hückel (1924) predicted $M_e = 2\varepsilon\zeta/3\eta$ for thick Debye layers ($\kappa R \ll 1$). These limits were bridged by Henry (1931), who calculated a monotonic increase in the magnitude of M_e with increasing κR. Importantly, M_e remains the same sign with varying κR for a fixed sign of ζ. For example, a negatively charged particle ($\zeta < 0$) has $M_e < 0$ for any κR and thus moves against $\boldsymbol{E}_\infty$ (to higher potentials).

O'Brien & White (1978) numerically solved the Poisson–Nernst–Planck (PNP) equations for point-like non-interacting ions to compute M_e over a wide range of ζ and κR. For $\kappa R \gg 1$ and $\zeta > 0$, M_e initially increases linearly with ζ according to Smoluchowski's result, then attains a maximum value for $\zeta \approx (5 - 10)k_BT/e$ and subsequently decreases to a finite value as $\zeta \to \infty$ (see also Dukhin & Deryaguin 1974; O'Brien 1983). More precisely, Smoluchowski's result holds until $\zeta \sim O[(k_BT/e)\ln(\kappa R)]$ (Schnitzer & Yariv 2012). The departure from Smoluchowski's prediction arises from surface conduction of ions in the Debye layer as a consequence of the exponentially large counterion concentration predicted by the PNP model at moderately large ζ. Khair & Squires (2009) showed that surface conduction can be reduced, and hence the mobility maximum can be delayed to unphysically large ζ, by inclusion of steric hindrance between finite sized ions using Bikerman's model (Bikerman 1942; Kilic, Bazant & Ajdari 2007*a*,*b*). Nonetheless, M_e retains the same sign with varying κR for a fixed sign of ζ.

However, 'mobility reversals' have been observed in experiments involving multivalent electrolytes with increasing salt concentration (Strauss, Gershfeld & Spiera 1954; Elimelech & O'Melia 1990; Martín-Molina *et al.* 2003; Quesada-Pèrez *et al.* 2005; Martín-Molina *et al.* 2009; Semenov *et al.* 2013). For example, at low ionic strength (small κR) a negatively charged particle ($\zeta < 0$) has $M_e < 0$ and migrates against $\boldsymbol{E}_\infty$ (to higher potentials). As ionic strength increases, M_e crosses zero and becomes positive – the particle migrates with $\boldsymbol{E}_\infty$ (to lower potentials). The abovementioned theories lack a key physical trait for capturing mobility reversals. Here, we present a continuum framework capable of predicting electrophoretic mobility reversals.

Concentrated electrolytes are known to exhibit 'overscreening', where the charge on a surface is overcompensated by a first layer of counterions, that first layer is overcompensated by a second layer consisting of coions, and so on; the ionic charge density oscillates in sign away from the surface (Mezger *et al.* 2008). A purported cause of overscreening is ion–ion electrostatic (Coulomb) correlations, beyond mean-field Debye screening (Grosberg, Nguyen & Shklovskii 2002; Levin 2002). Molecular dynamics (MD) and Monte Carlo (MC) simulations (Torrie & Valleau 1980; Fedorov & Kornyshev 2008), integral equation approaches (Gonzales-Tovar, Lozada-Cassou & Henderson 1985; Kjellander & Marcelja 1986; Attard, Mitchell & Ninham 1988; Ennis, Marcelja & Kjellander 1996; Martín-Molina *et al.* 2003) and density functional and statistical field theories (Netz & Orland 2000; Hatlo & Lue 2010; Gillespie *et al.* 2011) have predicted overscreening in equilibrium Debye layers. These techniques often adopt the primitive model of electrolytes as charged hard spheres in a dielectric continuum. Although they offer an accurate picture of the equilibrium Debye layer around simple geometries such as a flat plate or sphere,

https://doi.org/10.1017/jfm.2014.354 Published online by Cambridge University Press

calculation of electrophoretic mobility is challenging since the Debye layer is driven away from equilibrium by the imposed electric field. Martín-Molina *et al.* (2008) calculated the mobility of a spherical colloid using Smoluchowski's formula with ζ determined from an MC simulation for a flat plate that included Coulombic potentials for ion–ion and ion–wall interactions. Lozada-Cassou, González-Tovar & Olivares (1999) used the weak-field linearization of O'Brien & White (1978) along with an integral equation description of the equilibrium Debye layer around a spherical particle. Raafatnia *et al.* (2014) also utilized the weak-field linearization combined with MD simulation of the equilibrium Debye layer over a flat plate. While these approaches can predict electrophoretic mobility reversals, the first (Martín-Molina *et al.* 2008) does not account for surface conduction, and all three can become computationally intensive in complex geometries. Our approach below utilizes an entirely continuum framework, which could be applied to a wide range of particle geometries and is not restricted to the thin-Debye-layer limit.

Bazant, Storey & Kornyshev (2011) recently derived a modified Poisson equation (MPE) to capture ion–ion electrostatic correlations in equilibrium Debye layers (see also Santangelo 2006; Hatlo & Lue 2010). The MPE introduces a correlation length, ℓ_c, which is expected to be bounded from below by the ion diameter, a, and from above by $z_+^2\ell_B$, where $\ell_B = e^2/4\pi\varepsilon k_B T$ is the Bjerrum length, which signifies the distance at which the electrostatic energy between a pair of monovalent ions equals the thermal energy; in water, $\ell_B \approx 0.7$ nm. Ions separated by a distance greater than ℓ_c predominantly experience mean-field (screened) electrostatics; ions closer than ℓ_c experience (Coulombic) electrostatic correlations. The MPE reads $\varepsilon(\ell_c^2\nabla^4\varphi - \nabla^2\varphi) = \rho$, where φ is the electrostatic potential and $\rho = e(z_+n_+ + z_-n_-)$ is the ionic charge density, with n_+ and n_- the number densities of cations and anions, respectively. As suggested by Bazant *et al.* (2011), the MPE can be interpreted in terms of a permittivity operator $\hat{\varepsilon} = \varepsilon(1 - \ell_c^2\nabla^2)$ resulting from non-local dielectric responses of correlated ion pairs. The MPE can predict overscreening and an electro-osmotic flow reversal over a flat plate (Storey & Bazant 2012).

In § 2, we utilize the MPE to compute the mobility of a weakly charged (small ζ) particle. In § 3, we compute the mobility at larger ζ, using the MPE to describe electrostatic correlations and Bikerman's model to capture steric hindrance between ions. Conclusions are offered in § 4.

2. Electrophoretic mobility at small ζ

Consider a uniformly charged spherical colloid of radius R in a binary electrolyte. The charge density $\rho \approx -e^2n_+^\infty z_+(z_+ - z_-)\varphi/k_BT$ for $|\zeta| \lesssim k_BT/e$. Normalizing ρ by $z_+en_+^\infty$ and φ and ζ by k_BT/e, we obtain $\tilde{\rho} = -(z_+ - z_-)\tilde{\varphi}$, where we use a tilde to denote the dimensionless counterpart of a dimensional quantity. The radial distance, r, from the centre of the colloid is scaled by R and the dimensionless correlation length is $\delta_c = \ell_c\kappa$. The MPE thus reduces to a modified Debye–Hückel equation (for $\delta_c = 0$, the standard Debye–Hückel equation is recovered),

$$(\kappa R)^2\tilde{\nabla}^2\tilde{\varphi} - \delta_c^2\tilde{\nabla}^4\tilde{\varphi} = (\kappa R)^4\tilde{\varphi}. \tag{2.1}$$

As in Bazant *et al.* (2011) and Storey & Bazant (2012), $\tilde{\varphi}$ and its derivatives vanish as $\tilde{r} \to \infty$; $\tilde{\varphi} = \tilde{\zeta}$ and $\hat{\boldsymbol{n}} \cdot \tilde{\boldsymbol{\nabla}}(\tilde{\nabla}^2\tilde{\varphi}) = 0$ at $\tilde{r} = 1$, where $\hat{\boldsymbol{n}}$ is the unit vector normal to the surface. This last boundary condition assumes that correlations at the particle surface are negligible and yields predictions in agreement with molecular simulations (Bazant *et al.* 2011; Bazant, Storey & Kornyshev 2012; Storey & Bazant 2012).

https://doi.org/10.1017/jfm.2014.354 Published online by Cambridge University Press

Since the equilibrium potential is spherically symmetric, let $\tilde{\varphi} = \tilde{\zeta} f(\tilde{r})/\tilde{r}$. Thus, (2.1) reduces to $(\kappa R)^2 f'' - \delta_c^2 f'''' = (\kappa R)^4 f$, where primes denote derivatives in $\tilde{r}$. An analytical solution is readily obtained whose features are similar to the solution over a charged plate (Storey & Bazant 2012). Two distinct solutions exist based on the value of δ_c. For $\delta_c < 1/2$ ('weak correlations'), we arrive at

$$f(\tilde{r}) = A\mathrm{e}^{-n_1(\tilde{r}-1)} + (1-A)\mathrm{e}^{-n_2(\tilde{r}-1)}, \tag{2.2a}$$

where

$$n_1 = \frac{\kappa R}{\delta_c}\sqrt{\frac{1+\sqrt{1-4\delta_c^2}}{2}}, \quad n_2 = \frac{\kappa R}{\delta_c}\sqrt{\frac{1-\sqrt{1-4\delta_c^2}}{2}}, \quad A = \frac{n_2^2(n_2+1)}{n_2^2(n_2+1) - n_1^2(n_1+1)}, \tag{2.2b–d}$$

and for $\delta_c > 1/2$ ('strong correlations'), we arrive at

$$f(\tilde{r}) = \mathrm{e}^{-k_1(\tilde{r}-1)}[\cos(k_2(\tilde{r}-1)) + B\sin(k_2(\tilde{r}-1))], \tag{2.3a}$$

where

$$k_1 = \kappa R\frac{\sqrt{2\delta_c+1}}{2\delta_c}, \quad k_2 = \kappa R\frac{\sqrt{2\delta_c-1}}{2\delta_c}, \quad B = \frac{k_1^2(k_1+1) - k_2^2(3k_1+1)}{k_1k_2(3k_1+2) - k_2^3}. \tag{2.3b–d}$$

For weak correlations (2.2a–d), $f(\tilde{r})$ is the sum of exponentially decaying terms, resulting in a potential whose decay is monotonic with increasing $\tilde{r}$ yet predicts a greater potential near the surface than the case of $\delta_c = 0$. For strong correlations (2.3a–d), the potential has decaying oscillations, signifying charge inversion and stronger overscreening. From the definition of k_1 and k_2 in (2.3b–d) it is seen that $\sqrt{\ell_c/\kappa}$ is a more appropriate length scale to characterize charge density variation in a Debye layer with strong electrostatic correlations.

Figure 1 shows the dimensionless charge density $\tilde{\rho}$ versus $\tilde{r}$ for four combinations of κR and δ_c. For $\delta_c = 0$ and $\kappa R = 10$, $\tilde{\rho}$ decays monotonically to zero with increasing $\tilde{r}$. For $\delta_c = 5$ and $\kappa R = 10$, $\tilde{\rho}$ is larger (compared with $\delta_c = 0$) near the surface, indicating overscreening. To balance this excess counterion charge, coions are brought into the Debye layer and result in charge inversion – net negative charge density ($\tilde{\rho} < 0$) – seen at $\tilde{r} \sim 1.5$. At $\kappa R = 50$, a smaller Debye length, the same trend is observed, although the charge density decays more rapidly with $\tilde{r}$.

2.1. *Electrophoretic mobility*

An applied electric field, $\boldsymbol{E}_\infty$, sets the colloid into motion with an electrophoretic velocity $\boldsymbol{U}$. For small zeta potentials, $|\tilde{\zeta}| \lesssim 1$, polarization of the Debye layer can be neglected to a first approximation (Russel *et al.* 1989). Hence, the imposed field exerts an electrical force $\boldsymbol{F}_E$ on the colloid equal to $Q\boldsymbol{E}_\infty$, where $Q = 4\pi R\varepsilon\zeta$ $[f(1) - f'(1)]$ is the colloid surface charge. This expression for Q follows from the modified electrostatic boundary condition $\hat{\boldsymbol{n}} \cdot \boldsymbol{D} = q$, where $\boldsymbol{D} = -\hat{\varepsilon}\nabla\phi$ is the displacement field and q is the surface charge density, and the assumption $\hat{\boldsymbol{n}} \cdot \boldsymbol{\nabla}(\nabla^2\phi) = 0$ at the particle surface (Bazant *et al.* 2011). The fluid within the Debye layer undergoes an electro-osmotic flow, imparting a hydrodynamic force on the colloid, $\boldsymbol{F}_O = \int \rho\boldsymbol{P} \cdot \boldsymbol{E}\mathrm{d}V$, where $\boldsymbol{E} = [(1 + R^3/2r^3)\boldsymbol{I} - (3R^3/2r^3)\hat{\boldsymbol{r}}\hat{\boldsymbol{r}}] \cdot \boldsymbol{E}_\infty$ is the field around the insulating particle, $\boldsymbol{P} = (3R/4r + R^3/4r^3)\boldsymbol{I} + (3R/4r - 3R^3/4r^3)\hat{\boldsymbol{r}}\hat{\boldsymbol{r}}$ ($\boldsymbol{I}$ is

https://doi.org/10.1017/jfm.2014.354 Published online by Cambridge University Press

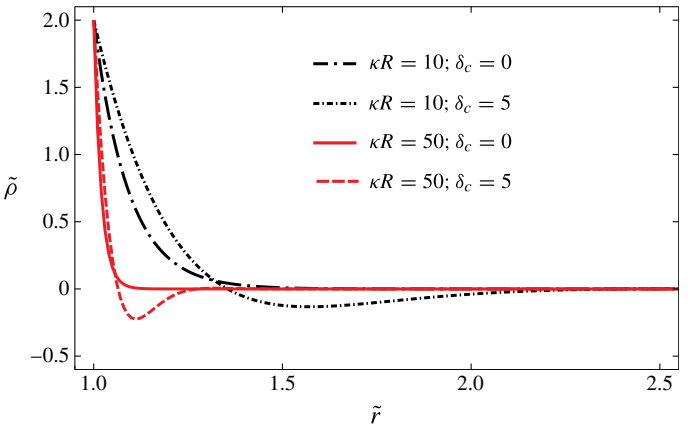


FIGURE 1. The dimensionless charge density, $\tilde{\rho}$, calculated from (2.1) for a monovalent electrolyte around a negatively charged sphere with $|\tilde{\zeta}| \lesssim 1$. Ion–ion electrostatic correlations ($\delta_c = 5$) lead to overscreening and charge oscillations.

the identity tensor and $\hat{\boldsymbol{r}}$ is a radial unit vector) and the integral is over the electrolyte volume. It should be noted that the expression for $\boldsymbol{F}_O$ is derived using the Lorentz reciprocal theorem in which the primary flow of interest is that due to a body force density $\rho\boldsymbol{E}$, resulting in the hydrodynamic force $\boldsymbol{F}_O$ on the colloid. The secondary flow in the reciprocal theorem is that due to an uncharged sphere translating at unit velocity, for which the tensor $\boldsymbol{P}$ relates the fluid velocity field to the velocity of the particle (see, e.g., Kim & Karrila 2005). The migration of the colloid results in a drag force, $\boldsymbol{F}_D = -6\pi\eta R\boldsymbol{U}$. Since the colloid is freely suspended, $\boldsymbol{F}_E$, $\boldsymbol{F}_O$ and $\boldsymbol{F}_D$ sum to zero; hence $\boldsymbol{U} = M_e\boldsymbol{E}_\infty$ and the dimensionless mobility, $\tilde{M}_e = 3\eta M_e/2\varepsilon\zeta$, is given by

$$\tilde{M}_e = -\frac{\mathrm{d}}{\mathrm{d}\tilde{r}}\left(\frac{f}{\tilde{r}}\right)\bigg|_{\tilde{r}=1} - (\kappa R)^2\int_1^\infty f(\tilde{r})\left(1 - \frac{1}{4\tilde{r}^3} + \frac{1}{4\tilde{r}^5}\right)\mathrm{d}\tilde{r}, \tag{2.4}$$

where the first term in (2.4) is a measure of the electrical force, $\boldsymbol{F}_E$, and the second term represents the electro-osmotic force, $\boldsymbol{F}_O$. After substituting the expressions for f given by (2.2*a–d*) into (2.4), we obtain for $\delta_c < 1/2$

$$\tilde{M}_e = (1 + A(n_1 - n_2) + n_2) - (\kappa R)^2(A\mathrm{G}_1 + (1 - A)\mathrm{G}_2), \tag{2.5a}$$

where

$$\mathrm{G}_x = \frac{1}{n_x} + \frac{\mathrm{e}^{n_x}}{4}\left(E_5(n_x) - E_3(n_x)\right), \tag{2.5b}$$

and for $\delta_c > 1/2$

$$\tilde{M}_e = (1 + k_1 - Bk_2) - (\kappa R)^2\left(\frac{k_1 + Bk_2}{k_1^2 + k_2^2} + \frac{1}{8}\left[(1 - B\mathrm{i})\mathrm{H}_1 + (1 + B\mathrm{i})\mathrm{H}_2\right]\right), \tag{2.6a}$$

where

$$\mathrm{H}_x = \mathrm{e}^{m_x}(\mathrm{E}_5(m_x) - \mathrm{E}_3(m_x)). \tag{2.6b}$$

https://doi.org/10.1017/jfm.2014.354 Published online by Cambridge University Press

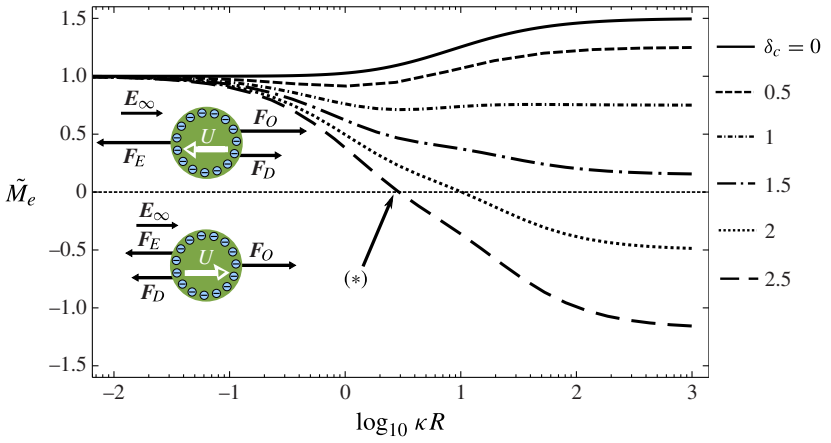


FIGURE 2. The electrophoretic mobility, $\tilde{M}_e = 3\eta M_e/2\varepsilon\zeta$, versus κR for various δ_c at small $\tilde{\zeta}$. The insets illustrate the direction and relative magnitudes of the electrical ($\boldsymbol{F}_E$), electro-osmotic ($\boldsymbol{F}_O$) and drag ($\boldsymbol{F}_D$) forces on a spherical colloid for $\tilde{M}_e > 0$ and $\tilde{M}_e < 0$ (reversals). At the point (∗) along the $\delta_c = 2.5$ curve, $\kappa R = 2.92$, and the mobility is close to zero, $\tilde{M}_e = 0.00020$, while the charge is of order unity, $Q/4\pi R\varepsilon\zeta = 2.72$. Thus, the points of zero charge and zero mobility do not coincide.

Here, $\mathrm{E}_a(z) = \int_1^\infty \mathrm{e}^{-z\tilde{r}}/\tilde{r}^a \mathrm{d}\tilde{r}$ is the exponential integral, $m_1 = k_1 - \mathrm{i}k_2$, $m_2 = k_1 + \mathrm{i}k_2$ and $\mathrm{i} = \sqrt{-1}$. It should be noted that $\mathrm{E}_a(z) = z^{a-1}\Gamma_u(1-a, z)$, where $\Gamma_u(v, z) = \int_z^\infty \mathrm{e}^{-\tilde{r}}\tilde{r}^{v-1}\mathrm{d}\tilde{r}$ is the upper incomplete Gamma function. In (2.5*b*) and (2.6*b*) the subscript x stands for either index 1 or 2. Despite the appearance of the imaginary unit in (2.6), the computed mobility is of course still real.

Because $\tilde{M}_e$ is normalized by ζ, reversals in mobility are signified by $\tilde{M}_e < 0$. The mobility is shown in figure 2 versus κR for various δ_c. For $\delta_c = 0$, $\tilde{M}_e$ increases monotonically from 1 to 1.5 with increasing κR (Henry 1931). For a negatively charged colloid (inset to figure 2), $\boldsymbol{F}_E$ is directed against the field and $\boldsymbol{F}_O$ is with the field (due to positive charge density in the Debye layer). There is an imbalance, $|\boldsymbol{F}_E| > |\boldsymbol{F}_O|$, so $\boldsymbol{F}_D$ must be with the field to balance the forces; thus, the particle migrates against the field: $\tilde{M}_e > 0$. As δ_c is increased at fixed κR (say $\kappa R = 10$ in figure 2), Q decreases and consequently the total charge in the diffuse layer, $\int \tilde{\rho}\mathrm{d}\tilde{V}$, decreases despite the overscreening causing more ions to be present. The lower Q and reduced diffuse charge result in lower $|\boldsymbol{F}_E|$ and $|\boldsymbol{F}_O|$, respectively. More precisely, $|\boldsymbol{F}_O|$ decreases due to a reduction in local charge density within the Debye layer by excess coions (figure 1), and hence a locally reduced electro-osmotic flow. (The no-slip condition prevents the excess counterions near the surface from driving a comparably enhanced electro-osmotic flow.) The rates of decrease of $|\boldsymbol{F}_O|$ and $|\boldsymbol{F}_E|$ are unequal, and $|\boldsymbol{F}_E| < |\boldsymbol{F}_O|$ for sufficiently large δ_c, in which case $\boldsymbol{F}_D$ points against the applied field. This switch in $\boldsymbol{F}_D$ is an electrophoretic mobility reversal, $\tilde{M}_e < 0$: a negatively charged colloid moves with the applied field. For thick Debye layers ($\kappa R \to 0$), $\tilde{M}_e$ is independent of δ_c since the charge density becomes vanishingly small. It should be noted that $\tilde{M}_e > 0$ for $\delta_c = 1.5$, thus overscreening and charge oscillation do not necessarily lead to mobility reversals. Importantly, Q is not zero when $\tilde{M}_e = 0$; the mobility reversal does not coincide with the point of zero particle charge. Another example where the point of zero charge does not coincide with zero

https://doi.org/10.1017/jfm.2014.354 Published online by Cambridge University Press

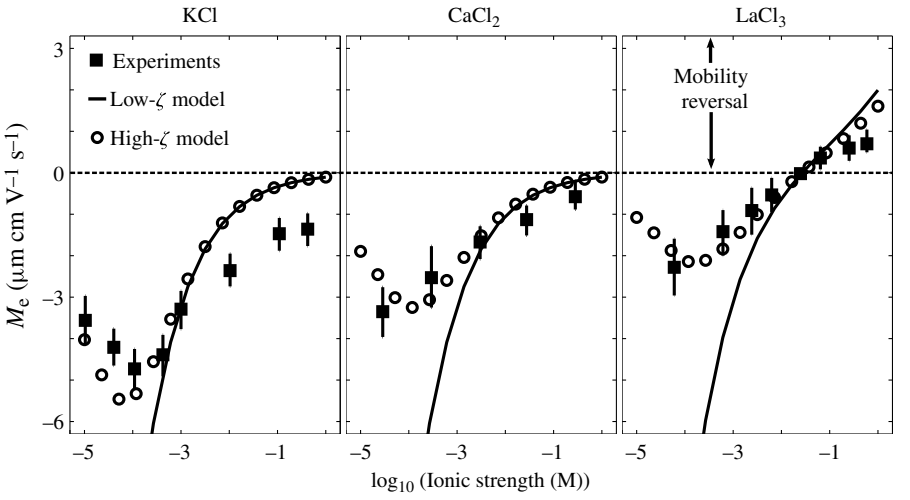


FIGURE 3. Theoretical predictions compared with experimental data taken from figure 5(*a*) of Semenov *et al.* (2013) (squares).

mobility is the non-zero induced-charge electrophoretic mobility of an uncharged metal particle under a uniform electric field in an asymmetric electrolyte (Bazant *et al.* 2009).

Figure 3 compares the mobility from (2.5)–(2.6) with experimental results of Semenov *et al.* (2013), who utilized optical tweezers to measure the electrophoretic velocity of a single polystyrene sulphonate latex colloid with a diameter of 2.23 μm. The colloid surface charge density was found by acid–base titration to be -0.31 μC cm^{-2} and is taken as constant at all concentrations. Experiments were performed in binary monovalent (KCl), divalent ($CaCl_2$) and trivalent ($LaCl_3$) salts; only the trivalent salt showed a mobility reversal. We chose the correlation length, ℓ_c, to best match the mobility in the high-concentration region for the mono- and divalent electrolytes, and to best match the concentration at which the mobility is zero in the trivalent electrolyte. For KCl and $CaCl_2$, $\ell_c = 0$. For $LaCl_3$, $\ell_c = 3.07$ nm, leading to $\delta_c = 0.03$ at the lowest ionic strength (0.01 mM, $\kappa R \sim 10$) and $\delta_c = 10.10$ at the highest one (1 M, $\kappa R \sim 3500$). This estimate of ℓ_c falls within the expected bounds of hydrated counterion diameter (0.49 nm) (Ohtaki & Radnai 1993) and $z_+^2 \ell_B$ (6.4 nm) for $LaCl_3$. It is remarkable that our simple analytical theory can capture the mobility reversal with a physically realistic value of ℓ_c. However, the theory overestimates $|M_e|$ at low ionic strengths. For $LaCl_3$ we predict $\tilde{\zeta} \approx -0.42$ at the reversal ($M_e = 0$), which is a suitably small zeta potential. At ionic strengths lower than $O(1$ mM$)$, $|\tilde{\zeta}|$ is sufficiently larger than unity to invalidate the small-zeta-potential theory.

3. Mobility at larger ζ

At larger $\tilde{\zeta}$, the applied field results in polarization of the Debye layer through ionic surface conduction. At the larger concentrations used in the experiments, surface conduction is expected to be mitigated by steric hindrance between ions (Khair & Squires 2009). Hence, we employ Bikerman's model (Bikerman 1942),

https://doi.org/10.1017/jfm.2014.354 Published online by Cambridge University Press

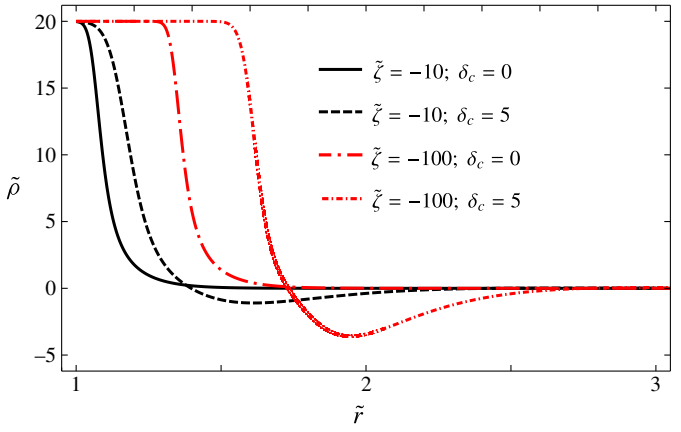


FIGURE 4. The dimensionless charge density $\tilde{\rho}$ of a monovalent electrolyte around a negatively charged sphere with $\kappa R = 10$ and bulk volume fraction $\nu = 0.1$. The counterions form an overscreening condensed layer, followed by a region of charge inversion due to coions. The extents of both grow with $|\tilde{\zeta}|$.

such that the electrochemical potential $\mu_\pm$, scaled by k_BT, of each ion species is $\tilde{\mu}_\pm = z_\pm\tilde{\varphi} + \ln n_\pm - \ln[1 - a^3(n_+ + n_-)]$, where the first two terms are for an ideal solution and the third term represents steric hindrance. The role of sterics is controlled by the bulk volume fraction of ions, $\nu = a^3(n_+^\infty + n_-^\infty)$, using a single ion size a (specified later). At equilibrium, $\tilde{\boldsymbol{\nabla}}\tilde{\mu}_\pm = 0$, which gives an explicit relationship between $\tilde{\varphi}$ and $\tilde{n}_\pm$ (the latter scaled by n_+^∞) (Kilic *et al.* 2007*a*) that is combined with the MPE to yield a 'Poisson–Fermi' equation (PFE) (Bazant *et al.* 2011) governing the equilibrium electrostatic potential,

$$\delta_c^2\tilde{\nabla}^4\tilde{\varphi} - (\kappa R)^2\tilde{\nabla}^2\tilde{\varphi} = (\kappa R)^4\beta(\tilde{\varphi})\frac{\mathrm{e}^{-z_+\tilde{\varphi}} - \mathrm{e}^{-z_-\tilde{\varphi}}}{z_+ - z_-}, \tag{3.1a}$$

where

$$\beta(\tilde{\varphi}) = \left(1 - \nu + \frac{\nu(z_+\mathrm{e}^{-z_-\tilde{\varphi}} - z_-\mathrm{e}^{-z_+\tilde{\varphi}})}{z_+ - z_-}\right)^{-1}. \tag{3.1b}$$

Figure 4 shows the dimensionless charge density, $\tilde{\rho} = \beta(\mathrm{e}^{-z_+\tilde{\varphi}} - \mathrm{e}^{-z_-\tilde{\varphi}})$, computed from (3.1) for a monovalent electrolyte at $\kappa R = 10$ and $\nu = 0.1$, for $\tilde{\zeta} = -10$ and -100. At such large $\tilde{\zeta}$, the counterions form a condensed layer at the surface due to steric hindrance. With correlations ($\delta_c \neq 0$), the condensed layer overscreens the surface charge and extends further from the surface, despite the Debye length remaining unchanged. The degree of overscreening by counterions and charge inversion due to coions increases with $\tilde{\zeta}$.

3.1. *Electrophoretic mobility: thin-Debye-layer analysis*

The electrolyte dynamics in response to a weak applied field is described by coupled linear equations governing the perturbations to the equilibrium electrochemical potentials, $\tilde{\mu}_\pm^1$, and fluid velocity, $\tilde{\boldsymbol{v}}^1$. The superscripts 0 and 1 indicate quantities that are zeroth or first order in the applied field (they are not meant to represent algebraic

https://doi.org/10.1017/jfm.2014.354 Published online by Cambridge University Press

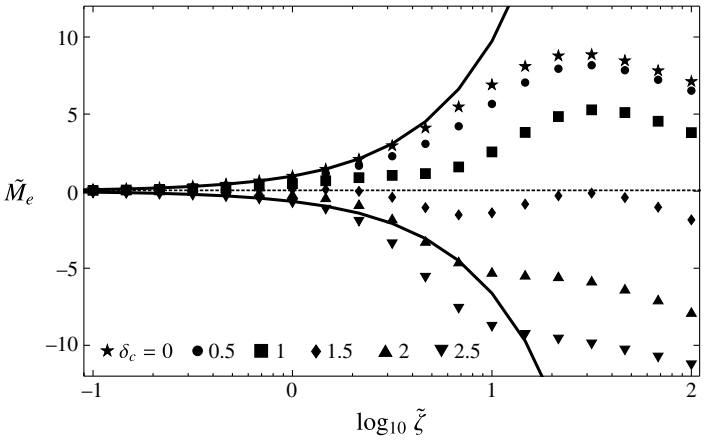


FIGURE 5. The dimensionless electrophoretic mobility, $\tilde{M}_e = \eta M_e/\varepsilon(k_BT/e)$, versus $\tilde{\zeta}$ for various δ_c with $\kappa R = 100$ and $\nu = 0.1$. The symbols are from solution of the large-$\tilde{\zeta}$ model (3.1)–(3.2) and the lines are from the small-$\tilde{\zeta}$ formulae (2.5*a*,*b*)–(2.6*a*,*b*) with $\delta_c = 0$ (top) and 2.5 (bottom).

powers). These equations are well known and read (O'Brien & White 1978; O'Brien 1983; Khair & Squires 2009)

$$\tilde{\nabla}^2\tilde{\mu}^1_\pm + \tilde{\nabla}\ln\tilde{n}^0_\pm \cdot \tilde{\nabla}\tilde{\mu}^1_\pm = \tfrac{1}{2}m\tilde{\boldsymbol{v}}^1 \cdot \tilde{\nabla}\ln\tilde{n}^0_\pm, \tag{3.2a}$$

$$\tilde{\nabla}^2(\tilde{\nabla}\times\tilde{\boldsymbol{v}}^1) = \frac{(\kappa R)^2}{\mathscr{Z}}(\tilde{\nabla}\tilde{n}^0_+ \times \tilde{\nabla}\tilde{\mu}^1_+ + \tilde{\nabla}\tilde{n}^0_- \times \tilde{\nabla}\tilde{\mu}^1_-), \tag{3.2b}$$

where $\mathscr{Z} = z_+(z_+ - z_-)$, and $\tilde{n}^0_+ = \beta e^{-z_+\tilde{\varphi}}$ and $\tilde{n}^0_- = -(z_+/z_-)\beta e^{-z_-\tilde{\varphi}}$ are the equilibrium cation and anion density, respectively, calculated from (3.1). The velocity field $\tilde{\boldsymbol{v}}^1$ is normalized by $\varepsilon(k_BT/e)^2/\eta R$, and $m = 2\varepsilon(k_BT/e)^2/\eta D$, with D a single ionic diffusion coefficient (specified later). Equation (3.2*a*) embodies ion conservation and (3.2*b*) governs the inertialess fluid flow with an electrochemical body force. It should be recalled that the experiments (Semenov *et al.* 2013) have $\kappa R \gg 1$. Therefore, a thin-Debye-layer asymptotic analysis is utilized to solve (3.2) and subsequently compute the mobility. The analysis is essentially identical to that of Khair & Squires (2009); details are not repeated here.

Figure 5 shows the dimensionless mobility, now defined as $\tilde{M}_e = \eta M_e/\varepsilon(k_BT/e)$, versus $\tilde{\zeta}$ for a positively charged particle in a monovalent electrolyte at various δ_c, for $\kappa R = 100$ and $\nu = 0.1$; our results agree with those of Khair & Squires (2009) for $\delta_c = 0$. The mobility computed from solution of (3.2) is in agreement with (2.5*a*,*b*)–(2.6*a*,*b*) at small $\tilde{\zeta}$. For $\delta_c = 0$, 0.5 and 1 the mobility does not reverse ($\tilde{M}_e > 0$), and surface conduction reduces the mobility relative to (2.5*a*,*b*)–(2.6*a*,*b*). A more complicated dependence of $\tilde{M}_e$ on $\tilde{\zeta}$ is observed when δ_c is sufficiently large for a mobility reversal to occur (e.g. $\delta_c = 1.5$).

Comparison of the large-ζ theory with experiments (Semenov *et al.* 2013) is shown in figure 3. The ion size a was taken to be the average of the hydrated ion diameters (Ohtaki & Radnai 1993), and D was calculated from the conductivity at infinite dilution (Vanýsek 2012). Again, $\ell_c = 0$ in KCl and $CaCl_2$, whereas now $\ell_c = 2.63$ nm

https://doi.org/10.1017/jfm.2014.354 Published online by Cambridge University Press

for $LaCl_3$, which is slightly lower than the estimate of 3.07 nm from the low-$\tilde{\zeta}$ model. The two models share the same agreement with the experiments at high concentrations, which is not surprising as $|\tilde{\zeta}| \lesssim 1$ there. The large-$\tilde{\zeta}$ model predicts $\tilde{\zeta} = -0.36$ at the mobility reversal in $LaCl_3$, compared with $\tilde{\zeta} = -0.42$ predicted from the low-$\tilde{\zeta}$ model. Notably, the large-$\tilde{\zeta}$ model shows better agreement with the experiments at lower concentration. Thus, Debye layer polarization must be accounted for to predict the mobility over a wide range of concentrations.

While we have included ion sterics through Bikerman's model, we note that this has little effect on the predicted mobility in figure 3, since when $|\tilde{\zeta}|$ is large enough to anticipate a reduction in surface conduction, the volume fraction, ν, is small due to the low ionic strength. Conversely, at higher ionic strengths when $\nu \sim O(0.1)$, $|\tilde{\zeta}| \lesssim 1$ and a condensed counterion layer does not form. Hence, we conclude that accounting for surface conduction is sufficient to improve agreement for large $|\tilde{\zeta}|$, at least for this range of concentrations and for these ions. Nevertheless, by accounting for correlations through the MPE, the prediction of electrophoretic mobility reversals is possible in both models.

4. Conclusions

A continuum framework to predict electrophoretic mobility reversals in concentrated multivalent electrolytes has been presented which incorporates ion–ion electrostatic correlations and steric hindrance between ions. Of course, additional effects are expected in concentrated systems, including local variations in viscosity and permittivity in the Debye layer (Bazant *et al.* 2009) and variation in bulk permittivity due to ion-specific polarizability (Hatlo, van Roij & Lue 2012). It should be recognized, however, that electrostatic correlations are the essential driver of mobility reversals. Raafatnia *et al.* (2014) utilized an attraction energy of $4k_BT$ between the counterion and the colloid surface to predict the observed mobility reversals in $LaCl_3$ (Semenov *et al.* 2013). In contrast, our work demonstrates that mobility reversals can be predicted solely from consideration of electrostatic ion–ion correlations in the diffuse Debye layer. Finally, the present approach can be adapted to predict a host of other electrokinetic phenomena in concentrated solutions, including dynamic (AC) electrophoresis, induced-charge electrophoresis, diffusiophoresis and dielectrophoresis.

Acknowledgements

We gratefully acknowledge the support of the Charles E. Kaufman Foundation of the Pittsburgh Foundation and NSF CAREER support under CBET-1350647.

References

Attard, P., Mitchell, D. J. & Ninham, B. W. 1988 Beyond Poisson Boltzmann: images and correlations in the electric double layer. I. Counterions only. *J. Chem. Phys.* **88**, 4987–4996.

Bazant, M. Z., Kilic, M. S., Storey, B. D. & Ajdari, A. 2009 Towards an understanding of induced-charge electrokinetics at large applied voltages in concentrated solutions. *Adv. Colloid Interface Sci.* **152**, 48–88.

Bazant, M. Z., Storey, B. D. & Kornyshev, A. A. 2011 Double layer in ionic liquids: overscreening versus crowding. *Phys. Rev. Lett.* **106**, 046102.

Bazant, M. Z., Storey, B. D. & Kornyshev, A. A. 2012 Erratum: Double layer in ionic liquids: overscreening versus crowding. *Phys. Rev. Lett.* **109**, 149903.

https://doi.org/10.1017/jfm.2014.354 Published online by Cambridge University Press

BIKERMAN, J. J. 1942 XXXIX. Structure and capacity of electrical double layer. *Phil. Mag.* **33**, 384–397.

DORFMAN, K. D. 2010 DNA electrophoresis in microfabricated devices. *Rev. Mod. Phys.* **82**, 2903–2947.

DUKHIN, S. S. & DERYAGUIN, B. V. 1974 Electrokinetic phenomena. In *Surface and Colloid Science* (ed. E. Matijevic), vol. 7. Wiley.

ELBASHIR, A. A. & ABOUL-ENEIN, H. Y. 2013 Capillary electrophoresis and molecular modeling as a complementary technique for chiral recognition mechanism. *Crit. Rev. Anal. Chem.* **43**, 131–137.

ELIMELECH, M. & O'MELIA, C. R. 1990 Effect of electrolyte type on the electrophoretic mobility of polystyrene latex colloids. *Colloid Surf.* **44**, 165–178.

ENNIS, J., MARCELJA, S. & KJELLANDER, R. 1996 Effective surface charge for symmetric electrolytes in the primitive model double layer. *Electrochim. Acta* **41**, 2115–2124.

FEDOROV, M. V. & KORNYSHEV, A. A. 2008 Ionic liquid near a charged wall: structure and capacitance of the electrical double-layer. *J. Phys. Chem.* B **112**, 11868–11872.

GILLESPIE, D., KHAIR, A. S., BARDHAN, J. P. & PENNATHUR, S. 2011 Efficiently accounting for ion correlations in electrokinetic nanofluidic devices using density functional theory. *J. Colloid Interface Sci.* **359**, 520–529.

GONZALES-TOVAR, E., LOZADA-CASSOU, M. & HENDERSON, D. 1985 Hypernetted chain approximation for the distribution of ions around a cylindrical electrode. II. Numerical solution for a model cylindrical polyelectrolyte. *J. Chem. Phys.* **83**, 361–372.

GROSBERG, A. Y., NGUYEN, T. T. & SHKLOVSKII, B. I. 2002 Colloquium: the physics of charge inversion in chemical and biological systems. *Rev. Mod. Phys.* **74**, 329–345.

HATLO, M. M. & LUE, L. 2010 Electrostatic interactions of charged bodies from the weak- to the strong-coupling regime. *Europhys. Lett.* **89**, 25002.

HATLO, M. M., VAN ROIJ, R. & LUE, L. 2012 The electric double layer at high surface potentials: the influence of excess ion polarizability. *Europhys. Lett.* **89**, 28010.

HENRY, D. C. 1931 The cataphoresis of suspended particles. Part I. The equation of cataphoresis. *Proc. R. Soc. Lond.* A **133**, 106–129.

HÜCKEL, E. 1924 Die Kataphorese der Kugel. *Phys. Z.* **25**, 204–210.

KHAIR, A. S. & SQUIRES, T. M. 2009 Ion steric effects on electrophoresis of a colloidal particle. *J. Fluid Mech.* **640**, 343–356.

KILIC, M. S., BAZANT, M. Z. & AJDARI, A. 2007*a* Steric effects in the dynamics of electrolytes at large applied voltages. I. Double-layer charging. *Phys. Rev.* E **75**, 021502.

KILIC, M. S., BAZANT, M. Z. & AJDARI, A. 2007*b* Steric effects in the dynamics of electrolytes at large applied voltages. II. Modified Poisson–Nernst–Planck equations. *Phys. Rev.* E **75**, 021503.

KIM, S. & KARRILA, S. J. 2005 *Microhydrodynamics: Principles and Selected Applications*. Dover.

KJELLANDER, R. & MARCELJA, S. 1986 Double-layer interaction in the primitive model and the corresponding Poisson–Boltzmann description. *J. Phys. Chem.* **90**, 1230–1232.

LEVIN, Y. 2002 Electrostatic correlations: from plasma to biology. *Rep. Prog. Phys.* **65**, 1577–1632.

LOZADA-CASSOU, M., GONZÁLEZ-TOVAR, E. & OLIVARES, W. 1999 Nonlinear effects in the electrophoresis of a spherical colloidal particle. *Phys. Rev.* E **60**, R17–R20.

MARTÍN-MOLINA, A., MAROTO-CENTENO, J. A., HIDALGO-ALVAREZ, R. & QUESADA-PÉREZ, M. 2008 Charge reversal in real colloids: experiments, theory and simulations. *Colloid Surf.* A **319**, 103–108.

MARTÍN-MOLINA, A., QUESADA-PÉREZ, M., GALISTEO-GONZÁLEZ, F. & HIDALGO-ÁLVAREZ, R. 2003 Looking into overcharging in model colloids through electrophoresis: asymmetric electrolytes. *J. Chem. Phys.* **118**, 4183–4189.

MARTÍN-MOLINA, A., RODRÍGUEZ-BEAS, C., HIDALGO-ÁLVAREZ, R. & QUESADA-PÉREZ, M. 2009 Effect of surface charge on colloidal charge reversal. *J. Phys. Chem.* B **113**, 6834–6839.

MEZGER, M., SCHRODER, H., REICHERT, H., SCHRAMM, S., OKASINSKI, J. S., SCHODER, S., HONKIMAKI, V., DEUTSCH, M., OCKO, B. M., RALSTON, J., ROHWERDER, M., STRATMANN, M. & DOSCH, H. 2008 Molecular layering of fluorinated ionic liquids at a charged sapphire (0001) surface. *Science* **322**, 424–428.

https://doi.org/10.1017/jfm.2014.354 Published online by Cambridge University Press

NETZ, R. R. & ORLAND, H. 2000 Beyond Poisson Boltzmann: fluctuation effects and correlation functions. *Eur. Phys. J.* E **1**, 203–214.

O'BRIEN, R. W. 1983 The solution of the electrokinetic equations for colloidal particles with thin double layers. *J. Colloid Interface Sci.* **92**, 204–216.

O'BRIEN, R. W. & WHITE, L. R. 1978 Electrophoretic mobility of a spherical colloid. *J. Chem. Soc. Faraday Trans. 2* **74**, 1607–1626.

OHTAKI, H. & RADNAI, T. 1993 Structure and dynamics of hydrated ions. *Chem. Rev.* **93**, 1157–1204.

QUESADA-PÈREZ, M., GONZÀLEZ-TOVAR, E., MARTÌN-MOLINA, A., LOZADA-CASSOU, M. & HIDALGO-ÀLVAREZ, R. 2005 Ion size correlations and charge reversal in real colloids. *Colloid Surf.* A **267**, 24–30.

RAAFATNIA, S., HICKEY, O. A., SEGA, M. & HOLM, C. 2014 Computing the electrophoretic mobility of large spherical colloids by combining explicit ion simulations with the standard electrokinetic model. *Langmuir* **30**, 1758–1767.

RUSSEL, W. B., SAVILLE, D. A. & SCHOWALTER, W. R. 1989 *Colloidal Dispersions*. Cambridge University Press.

SANTANGELO, C. D. 2006 Computing counterion densities at intermediate coupling. *Phys. Rev.* E **73**, 041512.

SCHNITZER, O. & YARIV, E. 2012 Macroscale description of electrokinetic flows at large zeta potentials: nonlinear surface conduction. *Phys. Rev.* E **86**, 021503.

SEMENOV, I., RAAFATNIA, S., SEGA, M., LOBASKIN, V., HOLM, C. & KREMER, F. 2013 Electrophoretic mobility and charge inversion of a colloidal particle studied by single-colloid electrophoresis and molecular dynamics simulations. *Phys. Rev.* E **87**, 022302.

SMOLUCHOWSKI, M. M. 1903 Contribution à la théorie de l'endosmose électrique et de quelques phenomènes corrélatifs. *Bull. Inst. Acad. Sci. Cracovie* **8**, 182–199.

SQUIRES, T. M. & QUAKE, S. R. 2005 Microfluidics: fluid physics at the nanoliter scale. *Rev. Mod. Phys.* **77**, 977–1026.

STOREY, B. D. & BAZANT, M. Z. 2012 Effects of electrostatic correlations on electrokinetic phenomena. *Phys. Rev.* E **86**, 056303.

STRAUSS, U. P., GERSHFELD, N. L. & SPIERA, H. 1954 Charge reversal of cationic poly-4-vinylpyridine derivatives in KBr solutions. *J. Am. Chem. Soc.* **76**, 5909–5911.

TORRIE, G. M. & VALLEAU, J. P. 1980 Electrical double layers. I. Monte Carlo study of a uniformly charged surface. *J. Chem. Phys.* **73**, 5807–5816.

VANÝSEK, P. 2012 *CRC Handbook of Chemistry and Physics*, 93rd edn (ed. W. M. Hayes), p. 5. CRC Press.

https://doi.org/10.1017/jfm.2014.354 Published online by Cambridge University Press